Contactless measurement of electrical conductivity for bulk nanostructured silver prepared by high-pressure torsion: A study of the dissipation process of giant strain

Masaki Mito, Keisuke Shibayama, Hiroyuki Deguchi, Kazuki Tsuruta, Takayuki Tajiri, Kaveh Edalati, and Zenji Horita

Citation: Journal of Applied Physics **122**, 125105 (2017); doi: 10.1063/1.4991430
View online: http://dx.doi.org/10.1063/1.4991430
View Table of Contents: http://aip.scitation.org/toc/jap/122/12
Published by the American Institute of Physics

Contactless measurement of electrical conductivity for bulk nanostructured silver prepared by high-pressure torsion: A study of the dissipation process of giant strain

Masaki Mito,[1,a)] Keisuke Shibayama,[1] Hiroyuki Deguchi,[1] Kazuki Tsuruta,[2] Takayuki Tajiri,[3] Kaveh Edalati,[4,5] and Zenji Horita[4,5]
[1]*Graduate School of Engineering, Kyushu Institute of Technology, Kitakyushu 804-8550, Japan*
[2]*Japan Synchrotron Radiation Research Institute (JASRI), Hyogo 679-5198, Japan*
[3]*Faculty of Science, Fukuoka University, Fukuoka 814-0180, Japan*
[4]*Department of Materials Science and Engineering, Faculty of Engineering, Kyushu University, Fukuoka 819-0395, Japan*
[5]*WPI, International Institute for Carbon-Neutral Energy Research (WPI-I2CNER), Kyushu University, Fukuoka 819-0395, Japan*

(Received 20 June 2017; accepted 12 September 2017; published online 26 September 2017)

We measured the electrical conductivity of bulk nanostructured silver prepared by high-pressure torsion (HPT) in a contactless manner by observing the AC magnetic susceptibility resulting from the eddy current, so that we could quantitatively analyze the dissipation process of the residual strain with sufficient time resolution as a function of temperature T and initial shear strain γ. The HPT process was performed at room temperature under a pressure of 6 GPa for revolutions $N = 0$–5, and we targeted a wide range of residual shear strains. The contactless measurement without electrode preparation enabled us to investigate both the fast and slow dissipation processes of the residual strain with sufficient time resolution, so that a systematic study of these processes became possible. The changes in the electrical conductivity as a function of N at room temperature were indeed consistent with changes in the Vickers microhardness; furthermore, they were also related to changes in structural parameters such as the preferred orientation, the interplanar distance, and the crystallite size. The dissipation process at $N = 1$, corresponding to $\gamma \approx 30$, was the largest and the fastest. For $N = 5$, corresponding to $\gamma \approx 140$, we considered the effects of grain boundaries, as well as those of dislocations. The strain dissipation was quite slow below $T = 290$ K. According to the analytical results, it became successful to conduct the quantitative evaluation of the strain dissipation at arbitrary temperatures: For instance, the relaxation times at $T = 280$ and 260 K were estimated to be 3.6 and 37 days, respectively. *Published by AIP Publishing.*
[http://dx.doi.org/10.1063/1.4991430]

I. INTRODUCTION

Diffusion physics occurs in many phenomena such as Brownian motion, mixtures of more than two components, atomic diffusion in hydrogen storage metals, and so on.[1] It remains an important subject, and understanding of the intrinsic physics requires the use of statistical physics.[1] As a phenomenon similar to that of diffusion, we pay much attention to the dissipation of strain in metals, because the dislocation moves and its density decreases as a function of time. Thus, the strain in a material, which is induced by severe stress such as dislocations, point defects, grain boundaries, stacking faults, and so on, dissipates. This dissipation is thermally activated, and it affects the mechanical strength of the material. Understanding the physics of such dissipation processes is extremely important for both kinetics and materials science.

Severe plastic deformation (SPD)[2,3] is achieved through a process such as high-pressure torsion (HPT),[4–7] equal-channel angular pressing,[8] accumulative roll bonding,[9,10] and so on. In particular, the SPD process plays a role in accumulating dislocations. Recently, significant grain refinement to the submicrometer or nanometer ranges has been reported to be well effective to create materials with good functionalities (e.g., high-strength materials).[11] Changes in the microstructure through SPD are often investigated by using scanning electron microscopy (SEM), transmission electron microscopy (TEM), Vickers microhardness (HV) measurements, and X-ray diffraction (XRD) analysis. Hardness is considered to be equivalent to the extent of blocking the dislocation motion. Indeed, hardness measurements are regarded as a standard technique to examine microstructural evolution with strain, and it is possible to reveal the occurrence of a steady state in HPT-processed metallic materials.[11] However, the aforementioned observations and measurements cannot be performed within a short time over wide ranges of time and temperature (especially at low temperatures), and so they are not suitable for quantitative analyses of fast or slow dissipation. Given these backgrounds, the electrical conductivity measurement that detects the scattering of conduction electrons is theoretically a useful approach to pursue the change in the microstructure such as dislocations, grain boundaries and lattice defects.[12,13] It is suitable for the study of fast and/or slow dissipation to

[a)]Electronic mail: mitoh@mns.kyutech.ac.jp

observe the voltage between two electrodes by using a digital voltmeter with sufficient sampling frequency. Indeed, four terminal methods for SPD materials have successfully been performed mainly for 300 and 77 K.[14–16] In the case of good metals, however, it is required to prepare long specimens, and so it is difficult to investigate the temperature dependence of electrical conductivity at low temperatures down to the liquid-helium temperature. Recently, electrical conductivity measurements by the scanning 4-point probe method have been used to evaluate microstructural homogeneity and crystal changes in HPT-processed Ti and Zr metals in the temperature ranges above 300 K.[17] It is not a suitable method to covering the low temperature region. The goal of this study is to investigate fast changes in the microstructure and the dissipation of residual strain over the wide temperature range. We adopt in this study a contactless approach without preparation of the electrode. There, we conduct magnetic measurements, where the temperature is controlled over a wide temperature range, so that we can also obtain knowledge of thermally activated dissipation for the accumulated strain.

The target material is silver (Ag) processed by HPT, hereafter denoted as HPT-Ag. The HPT-Ag has already been known to exhibit changes in HV within a few days after exposure at room temperature.[18] Ag has a face-centered cubic (fcc) structure, and its stacking fault energy is lower than that of similar fcc metals such as Cu and Au. Thus, the dislocation is difficult to annihilate and, after the formation of a small-angle grain-boundary, a large-angle grain boundary is constructed. Because electrical conductivity is a measure of the scattering of conduction electrons, it can be used to investigate changes in the HPT-Ag microstructure. However, changes in the microstructure at temperatures above room temperature occurred soon after the HPT processing, and the measurements need to be started without taking time to prepare four electrodes. The contactless approach is thus quite useful for such a requirement.[19] The results are then compared to the HV results and structural parameters. These results will be presented prior to describing the experimental data on electrical conductivity.

II. EXPERIMENTALS

A. Sample preparation

High-purity (99.99%) Ag discs with 10 mm diameter and 0.8 mm thickness were subjected to HPT processing at room temperature under a pressure of $P = 6$ GPa and revolutions $N = 0$–5 ($N = 0$, 1/16, 1/8, 1/4, 1/2, 1, 2, and 5) for the HV measurements.[5,6] For small N's, dislocations are stored with increasing N, and for large N's, the large-angle grain-boundaries are formed. For the electrical conductivity measurements, disks with 4 mm diameter were punched out from the above HPT-processed samples, whose center parts with 3 mm diameter were not used because of the creation of less shear strain.

The shear strain (γ) for the measurement points is estimated by

$$\gamma = 2\pi rN/h, \tag{1}$$

where r is the distance from the disc center and h is the thickness. When comparison is made for a series of data on strain dissipation with different r and h values, γ is more useful than N because it also varies with r.

Earlier studies on the HV measurement for $N = 5$ reported that the change in the hardness was minimal at a temperature (T) of 250 K, whereas at $T = 300$ K, it began to decrease after 1 day and reached the annealed level after more than 3 days.[18] SEM and TEM images of the specimen with $N = 5$ have already been presented elsewhere.[18] The grain-size decreased with HPT processing from a few tens of μm to 0.1 μm, and after HPT processing, grain coarsening occurs and the grain size gradually approaches 100 μm over time.

B. Vickers microhardness

As the first reference experiment, Vickers microhardness (HV) values for the $N = 1/4$, 1, and 5 samples at room temperature were measured within 1 h and up to 50 h after HPT processing. The measurements were conducted using a load of 200 gf at $r = 0.1$, 1.0, 2.0, 3.0, and 4.0 mm. A total of 30 hardness values were plotted as a function of γ to examine any change associated with the microstructure through stain dissipation which occurred over approximately two days.

C. XRD

As the second reference experiment, the XRD patterns for the specimen with $N = 5$ ($\gamma = 138.5$) at room temperature were measured every 15 min for 48 h by using a commercially available X-ray diffractometer (Rigaku SmartLab) with parallel beam optics. The incident X-rays were CuKα radiation. The four major diffraction peaks corresponding to the plane indices as (111), (200), (220) and (311) were measured by $2\theta/\theta$ scan, in which the scattering vector was always parallel to the surface normal. Only near the four diffraction peaks, the scanning was conducted to save time. The time required to measure each Bragg peak was approximately 3 min. For each of the diffraction peaks, the peak intensity, the peak angle, and the full width at half maximum (FWHM) were evaluated to estimate the degree of preferred orientation, the crystalline plane distance d, and the crystallite size D. For reference, the preferred orientation of the as-received specimen was (220). The preferred orientation just after HPT processing was (111).

D. Contactless electrical conductivity measurements

The electrical conductivity was measured by observing the AC response due to the eddy-current at frequencies (f) of up to 1 kHz. It is known that the AC response is normalized with the dimensionless frequency θ^2 as

$$\theta^2 = 2\pi f \mu_0 \sigma a^2, \tag{2}$$

where f is the frequency of the AC magnetic field H_{AC} ($= H \sin 2\pi ft$, where H is the AC field amplitude and t is the time), μ_0 is the permeability of free space, σ is the electrical conductivity, and a is the radius of the cylinder-shaped specimen.[20] On the right-hand side of Eq. (2), only σ is a

physical quantity as a function of temperature T. When the electrical conductivity of a targeted material with a constant a is studied as a function of T, the AC magnetic magnetization $M = A\sin(2\pi ft - \phi)$ is measured at a fixed T as a function of f. Here, A is the amplitude of the AC magnetic response and ϕ is the phase delay against the AC field.

In the present study, we measured the magnetization M under an AC magnetic field of $H = 3.9$ Oe and $f = 200$–1000 Hz for $T = 77$–300 K using a commercially available superconducting quantum interference device (SQUID) magnetometer (Quantum Design MPMS-5S), where SQUID was used as the sensing device to transform magnetic flux into voltage. The amplitude of time-dependent M was normalized with respect to the initial conductivity σ_0 at $t \approx 0$ s. This method was confirmed to be useful for detecting changes in σ due to strain dissipation in a previous study of Al subjected to accumulative roll bonding.[19] Then, M was normalized with that at the lowest measurement temperature (5 K), so that the temperature dependence of the relative σ could be obtained.

III. EXPERIMENTAL RESULTS

A. Mechanical and structural measurements

Prior to describing the results of σ, the mechanical and structural data are presented in order to understand the changes in σ. Figure 1 shows the change in HV of HPT-Ag with $N = 1/4$, 1, and 5 within 1 h and up to 50 h after HPT processing. For $\gamma > 4$, a change in HV between the above two states occurs. In particular, at approximately $\gamma = 20$–40, the change in HV reaches a maximum, where the dissipation accompanying the change in HV is the most prominent.

Figure 2 shows the XRD profiles for a representative specimen just after HPT and up to 48 h after HPT. As mentioned above, the preferred orientation just after HPT processing was (111). After 500 min, the magnitude of the orientation of (200) increased, as shown in Fig. 3. After 1000 min, the preferred orientation changed from (111) to (200) after HPT. Figure 4 shows the time dependence of structural parameters such as the interplanar distance (d) of the aforementioned crystal planes and the crystallite size (D) obtained from the peak position and the FWHM of these diffraction peaks in HPT-Ag for $N = 5$. Both d and D are normalized with the initial values at $t = 0$ (d_0 and D_0). As for (111) and (220), there are no significant changes with time. However, d and D for the (200) orientation begin to change at $t \approx 500$ min, and the changes tend to saturate at $t \approx 1500$ min (approximately 1 day). According to previous studies,[18] HV begins to decrease at $t \approx 1$ day. Thus, the change in HV is confirmed to be related to changes in the microstructure.

Subsections III B and III C demonstrate how the conduction electrons are influenced by the aforementioned changes in the structural feature as well as the mechanical property.

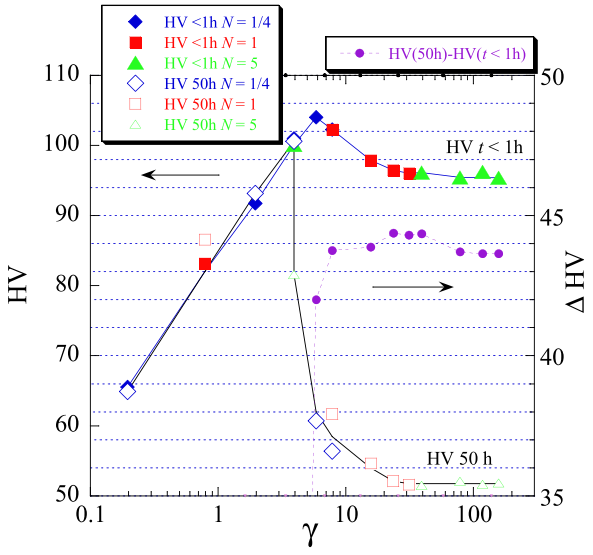

FIG. 1. Vickers microhardness (HV) values of HPT-Ag with $N = 1/4$, 1, and 5 in the states within 1 h and up to 50 h after HPT processing as a function of shear strain γ.

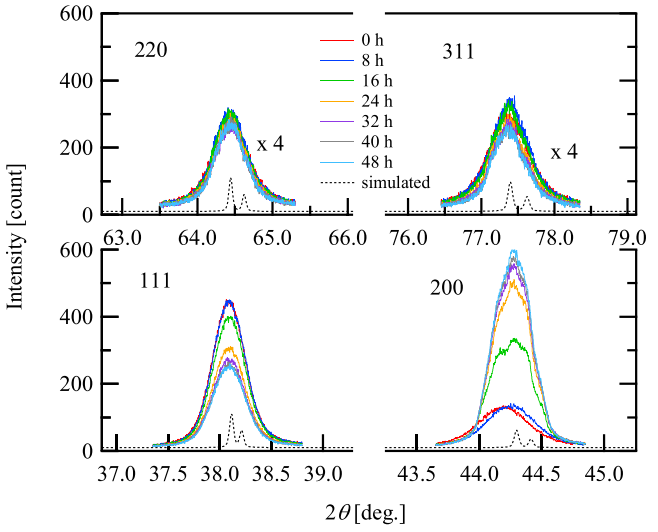

FIG. 2. XRD profiles of HPT-Ag ($P = 6$ GPa and $N = 5$) at room temperature in the states just after HPT processing and up to 48 h after HPT processing, together with the simulated profiles.

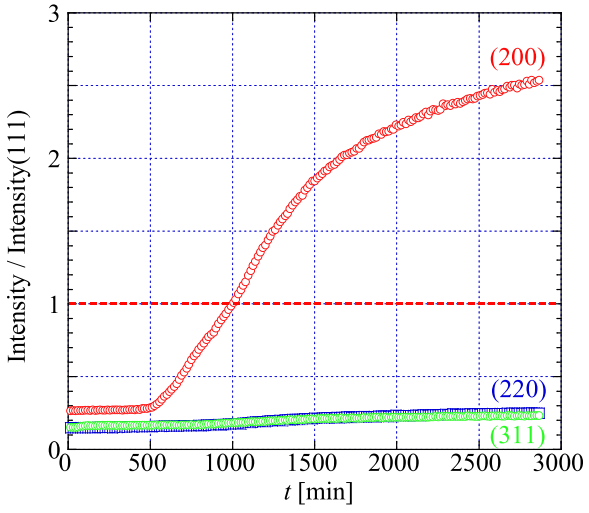

FIG. 3. Time dependence of preferred orientation of HPT-Ag for $P = 6$ GPa and $N = 5$.

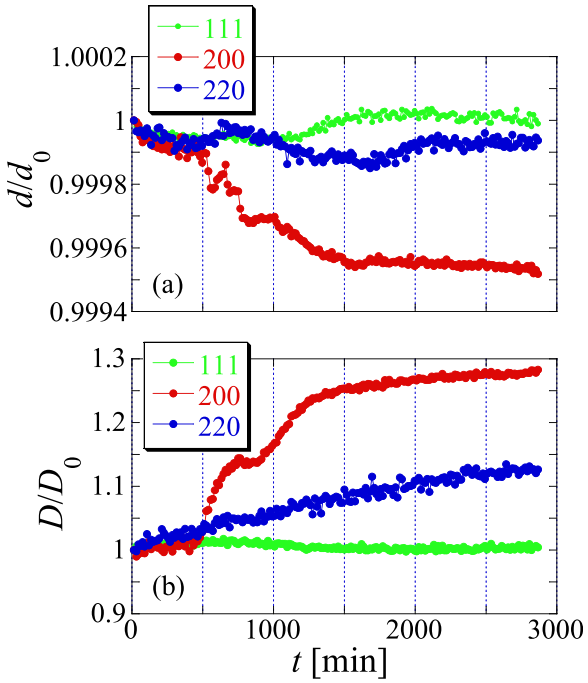

FIG. 4. Time dependence of structural parameters such as (a) the interplanar distance d of the aforementioned crystal planes and (b) the crystallite size D of HPT-Ag for $P = 6$ GPa and $N = 5$. Both d and D are normalized with their initial values at $t = 0$ (d_0 and D_0).

B. Contactless electrical conductivity: Strain dissipation at room temperature

Figure 5 shows the N dependence of the relative electrical conductivity σ/σ_0 for HPT-Ag at $T = 300$ K. The reference conductivity σ_0 is the conductivity at the initial time. There is a gradual change in σ/σ_0, even for the sample of $N = 0$ that experienced only pressing under $P = 6$ GPa. For $N = 1/16$, the change becomes slightly larger. However, in $N = 1/8$ ($\gamma \sim 3.4$), σ/σ_0 shows the time dependence characteristic of the relaxation process, the behavior of which is also described in Subsection III C. At $t \approx 700$ min, the relaxation starts, and at $t \approx 5500$ min, it levels off to a stationary state. For $N = 1/4$ ($\gamma \sim 7$), similar behavior occurs over a shorter time, and the magnitude of the change increases. For $N = 1/4 \rightarrow 1/2$, this change becomes more prominent. However, when the results for $N = 1/2$ ($\gamma \sim 13$) and $N = 5$ ($\gamma \sim 140$) are compared, the effect of N diminishes. A critical revolution number, N_c, may exist at $N = 1/2$–$3/2$, which corresponds to $\gamma = 20$–40.

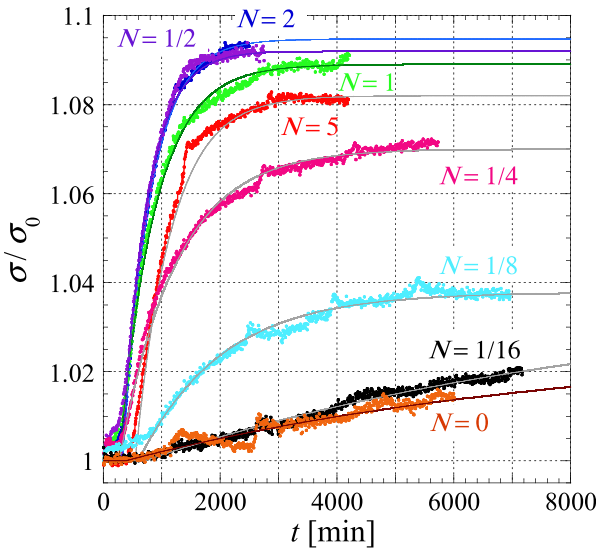

FIG. 5. Time and N dependence of relative electrical conductivity σ/σ_0 for HPT-Ag ($P = 6$ GPa) at $T = 300$ K.

Generally, the nucleation and growth process in metallurgy is expressed by a function $f(t)$ in the form of the Johnson-Mehl-Avrami (JMA) equation[21–23] as

$$f(t) = 1 - \exp(-Kt^n), \tag{3}$$

where K is a reaction rate constant and n (called the Avrami exponent) is a constant related to the behaviors of nucleation and growth.[24] This function is valid for understanding the phenomena such as metal recrystallization,[25,26] amorphous semiconductor crystallization,[25] and hydrogen storage (absorption and desorption).[27] The JMA equation includes the assumption that the growth rate of a new phase is controlled by temperature and is independent of time.[26] Indeed, the above behavior of hydrogen absorption and desorption is quite similar to that of the present strain dissipation,[27] so that we use the form of the JMA equation to analyze the present results. In this study, K corresponds to a dissipation rate of the strain.

Now, we investigate the change in σ/σ_0, so that the JMA equation is modified as

$$\frac{\sigma}{\sigma_0} = 1 + Af(t), \tag{4}$$

where A is the saturation value of the change. The data for $T = 290$–300 K exhibit a gradual change prior to the exponential change as mentioned later, and so they are reproduced well with the JMA equation with $n = 3$. However, for the data at $T > 300$ K without the former gradual change, the JMA equation with $n = 1$ rather than that with $n = 3$ becomes a better analytic formula. Therefore, we analyze a series of data using the following formula:

$$\frac{\sigma}{\sigma_0} = 1 + A\left(1 - \exp\left(-\frac{t - t_0}{\tau}\right)\right), \tag{5}$$

where t_0 is the incubation time and τ is the time constant of the relaxation.

Figure 6 shows the N and γ dependence of A, τ, and t_0 of Eq. (5) for HPT-Ag ($P = 6$ GPa) at $T = 300$ K. The strain dissipation in Ag is prominent for the specimen with a shear strain above approximately 5. These results are consistent with the aforementioned phenomenon explained for the HV results shown in Fig. 1. A has a maximum value at approximately $N_c = 1 \pm 0.5$, whereas τ and t_0 have minimum values. We have to consider the dissipation mechanism for $N < N_c$ and $N > N_c$, respectively. As mentioned above, at approximately $\gamma = 20$–40, the change in HV reaches a maximum. Indeed, N_c corresponds to $\gamma = 20$–40, showing consistency with the mechanical data. From the viewpoint of quantitative analysis, the electrical conductivity measurement exhibits better sensitivity than the HV measurement.

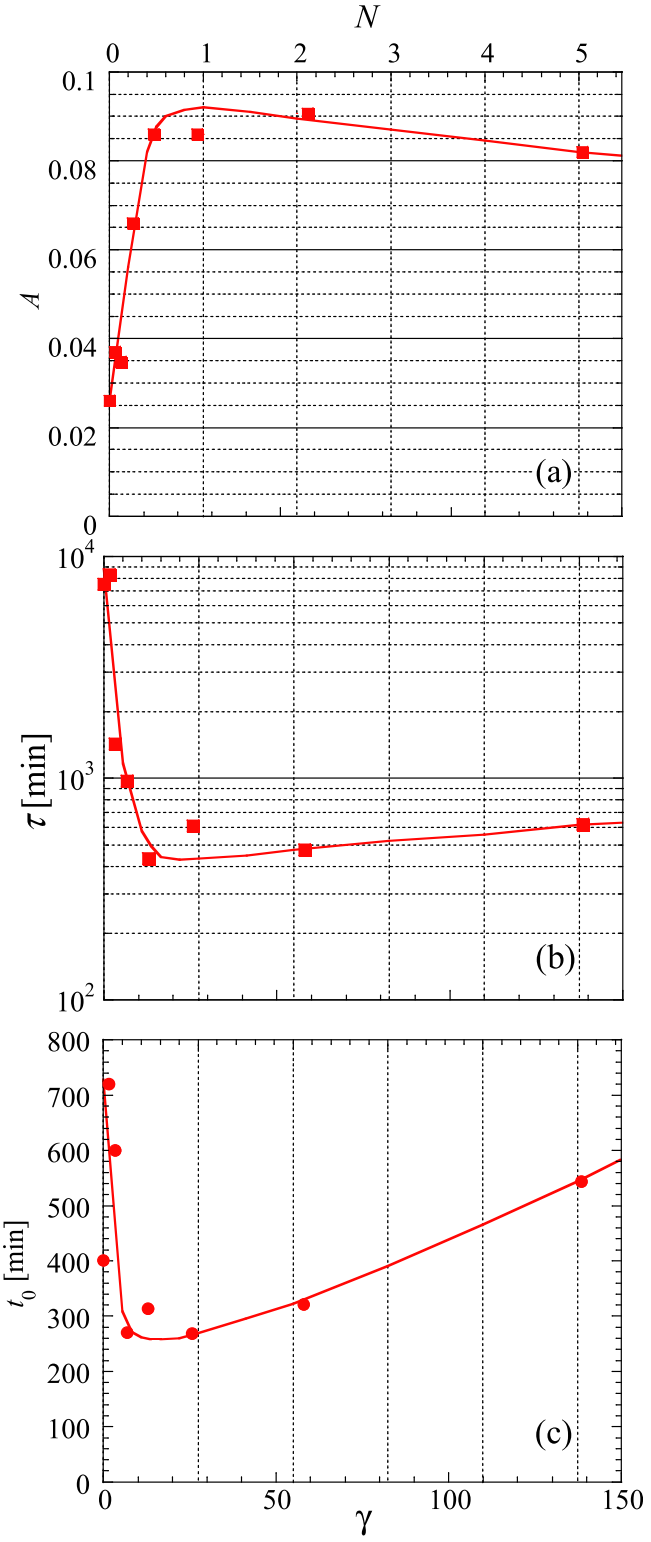

FIG. 6. N and γ dependence of A (a), τ (b), and t_0 (c) to characterize the N and γ dependence of the relative electrical conductivity σ/σ_0 for HPT-Ag ($P = 6$ GPa) at $T = 300$ K.

C. Contactless electrical conductivity: Temperature dependence of strain dissipation

Figure 7 shows the time dependence of relative electrical conductivity σ/σ_0 for HPT-Ag at $T = 290$–310 K. We also conducted similar measurements in the temperature (T) range from 77 K to 280 K, although the figure is not shown here. We confirmed that the data at $T = 77$ K remain unchanged up to 4 days and those at 280 K remain almost the same until at least 2 days.

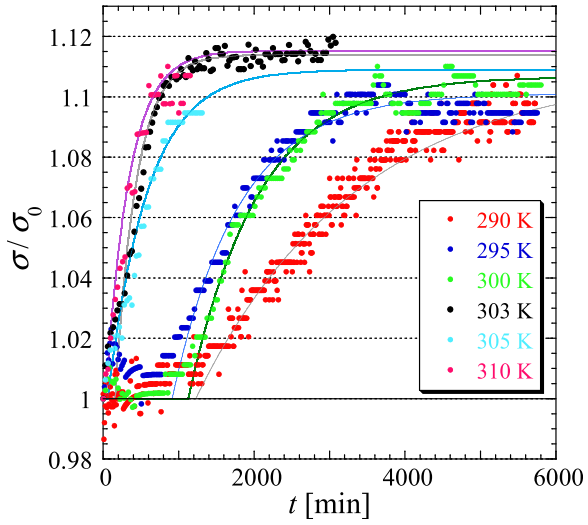

FIG. 7. Time and temperature dependence of relative electrical conductivity σ/σ_0 of HPT-Ag for $P = 6$ GPa and $N = 5$.

Figure 8 shows the T dependence of A, the relaxation time τ, and the incubation time t_0. First, as seen in Fig. 8(a), the value of A hardly changed as a function of T, and the saturated conductivity corresponds to the 11% increase in the initial conductivity. As seen in Fig. 8(b), both τ and t_0 depend on T. The relaxation time τ should follow the Arrhenius form in Ref. 26. Indeed, as seen in Fig. 8(c), the relaxation time τ varies according to the following Arrhenius plot:

$$\tau = \tau_0 \exp\left(\frac{\Delta}{k_B T}\right), \tag{6}$$

where the prefactor τ_0 is 3.39×10^{-10} min and the activation energy Δ/k_B is 8.50×10^3 K (k_B is the Boltzmann constant). Given these analytical results, the relaxation time at 260 and 280 K was 37 and 3.6 days, respectively, and that at 320 K was 2 h at most. As for the starting time of the relaxation, there might have been a discrete jump at approximately $T = 300$ K. Above 300 K, the dissipation started soon after raising the temperature to the target temperature for measurement. Below 300 K, there was an incubation time t_0 before the start of the dissipation process. We emphasize that the results of σ/σ_0 obtained at $T = 300$ K are consistent with the previous HV measurements.[18]

IV. DISCUSSION

In HPT processing, samples are subjected to a compressive force and concurrent torsional straining, so that the metal achieves exceptional grain refinement and exceptionally high strength. In pure Al[28] and pure Mg,[29] the hardness initially increases with increasing strain. The hardness reaches a maximum by further intense straining using HPT processing, and decreases to a constant level. Similar behavior was observed in the present HPT-processed Ag, as seen in Fig. 1. Thus, this

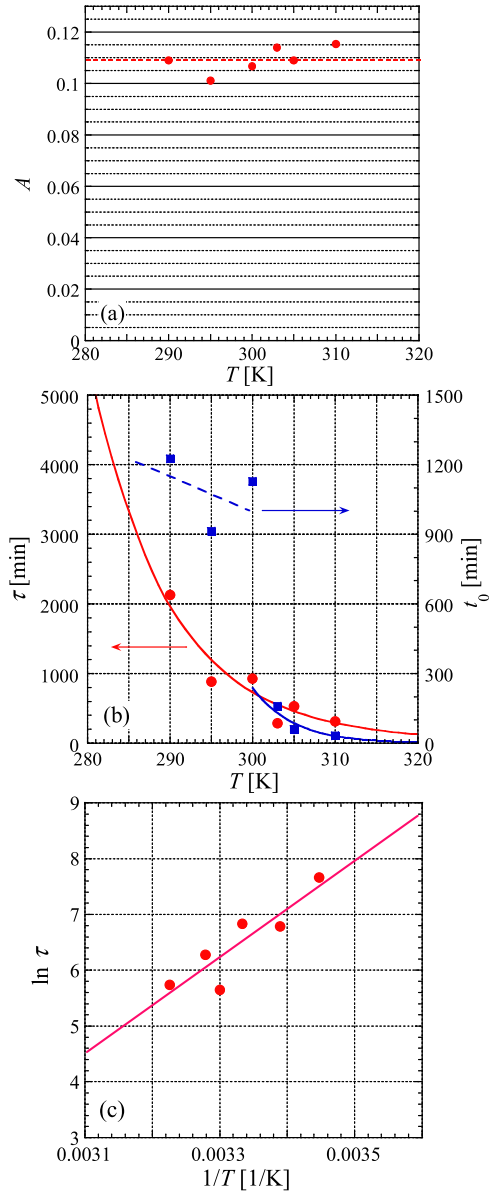

FIG. 8. Temperature dependence of (a) A and (b) τ and t_0 to characterize the temperature dependence of the relative electrical conductivity σ_r of HPT-Ag for $P = 6$ GPa and $N = 5$. (c) The data on τ in (b) are shown using the plot of $\ln \tau$ vs. $1/T$. The red dotted line in (a), the blue dashed line in (b), and the blue solid curve in (b) are visual guides. The red solid curve in (b) and the red solid line in (c) represent Eq. (6) with $\tau_0 = 3.39 \times 10^{-10}$ min and $\Delta/k_B = 8.50 \times 10^3$ K.

phenomenon is ascribed to the change in blocking the dislocation motion.

In the present Ag with low stacking fault energy, for $N < N_c$, the dissipation becomes prominent with increasing N. However, for $N > N_c$, the opposite is observed. This dissipation process is thermally activated and, for $N = 5$, it becomes appreciable at temperatures above 290 K. At room temperature, the TEM images for $N = 5$ show that the misorientation becomes distinctive.[18] We need to discuss some factors such as dislocations and grain boundaries to understand the changes in the electrical conductivity.[12] It is reasonable to consider the following scenario: For $N < N_c$, dissipation occurs for the strain due to dislocation stored in the process of grain refinement. However, for $N > N_c$, the dissipation may be retarded due to the formation of large-angle grain boundaries. In particular, the start of this dissipation occurs later, suggesting the enhancement of activation energy. Both the relaxation time and the change in electrical conductivity decrease slightly. The mismatch between grains with special orientation might create a kind of energy barrier to start the dissipation, resulting in the delay of dissipation.

Ag has a face-centered cubic (fcc) structure, and its stacking fault energy is lower than that of similar fcc metals such as Cu and Au. There, the storage of the dislocation is prominent for small shear strain. Furthermore, its good electrical conductivity helps us measure the AC magnetic susceptibility due to the eddy current. This situation is suitable for measuring the electrical conductivity over several days.

Au processed by HPT at room temperature shows relaxation within one month,[18] and Cu processed by HPT at cryogenic temperature shows relaxation in a few hours. If we pursue the strain dissipation in Cu and Au, we have to prepare sufficient machine time over one month for Au and perform HPT processing at the temperature as low as liquid nitrogen for Cu.

It is noted that the numerical analysis of the change in the electrical conductivity due to the dissipation process yielded quantitative results for the dissipation phenomenon, so that we could construct a scenario of the dissipation process such as strain-induced dissipation and dissipation combined with grain boundaries. In that sense, the electrical measurement using the scattering of conduction electrons is more convenient than the structural analyses using XRD, SEM and TEM.

V. CONCLUSION

Contactless electrical conductivity, which is a measure of the scattering of electrons, can be a useful approach for evaluating the change in the strained micro-structure. The benefit of this approach is that we do not have to prepare the electrodes, so that we can investigate fast dissipation processes as well as slow ones. By using a commercially available SQUID magnetometer, we can investigate the dissipation process over wide temperature ranges and long time scales. Because of good time resolution, we can evaluate the relation time. The present approach can yield a wealth of physical information on the strain dissipation process, together with SEM, TEM, and HV measurements. Furthermore, by analyzing the relaxation following the Arrhenius law, we can evaluate the time scale of the strain dissipation at arbitrary temperatures. According to the analytical prediction, in HPT-Ag, the dissipation times at 280 and 260 K were estimated to be 3.6 and 37 days, respectively.

The strain dissipation in Ag is prominent for samples with shear strains of more than 3, and it becomes active above 290 K. These behaviors are consistent with the phenomena observed in the mechanical measurements. According to the quantitative analysis of the dissipation process, we can distinguish the dissipation below a shear strain of 20–40 from that above the threshold. The former is the dissipation of dislocation, whereas the latter involves the dissipation of grain boundaries.

ACKNOWLEDGMENTS

This work was supported by MEXT KAKENHI, Grant-in-Aid for Scientific Research on Innovative Areas "Bulk Nanostructured Metals" No. 25102709, and Grant-in-Aid for Scientific Research (S) (No. 26220909). The HPT process was carried out in the International Research Center on Giant Straining for Advanced Materials (IRC-GSAM) at Kyushu University.

[1]H. Mehrer, *Diffusion in Solids* (Springer, Berlin, Heidelberg, New York, 2007).
[2]R. Valiev, Y. Estrin, Z. Horita, T. Langdon, M. Zehetbauer, and Y. Zhu, JOM **58**, 33 (2006).
[3]R. Valiev, R. Islamgaliev, and I. Alexandrov, Prog. Mater. Sci. **45**, 103 (2000).
[4]P. W. Bridgman, Phys. Rev. **48**, 825 (1935).
[5]N. A. Smirnova, V. I. Levit, V. I. Pilyugin, R. I. Kuznetsov, L. S. Davydova, and V. A. Sazonova, Fiz. Met. Metalloved. **61**, 1170 (1986).
[6]Y. Harai, Y. Ito, and Z. Horita, Scr. Mater. **58**, 469 (2008).
[7]K. Edalati and Z. Horita, Mater. Sci. Eng. A **652**, 325 (2016).
[8]V. M. Segal, V. I. Reznikov, A. E. Drobyshevskiy, and V. I. Kopylov, Russ. Metall. **1**, 99 (1981).
[9]A. Azushima, R. Kopp, A. Korhonen, D. Yang, F. Micari, G. Lahoti, P. Groche, J. Yanagimoto, N. Tsuji, A. Rosochowski *et al.*, CIRP Ann. Manuf. Tech. **57**, 716 (2008).
[10]Y. Saito, H. Utsunomiya, N. Tsuji, and T. Sakai, Acta Mater. **47**, 579 (1999).
[11]A. Zhilyaev and T. Langdon, Prog. Mater. Sci. **53**, 893 (2008).
[12]A. Karolik and A. Luhvich, J. Phys.: Condens. Matter **6**, 873 (1994).
[13]B. Watts, J. Phys. F: Met. Phys. **18**, 1197 (1988).
[14]Y. Miyajima, S. Komatsu, M. Mitsuhara, S. Hata, H. Nakashima, and N. Tsuji, Philos. Mag. **90**, 4475 (2010).
[15]Y. Miyajima, S. Komatsu, M. Mitsuhara, S. Hata, H. Nakashima, and N. Tsuji, Philos. Mag. **95**, 1139 (2015).
[16]A. M. Mavlyutov, A. S. Bondarenko, M. Y. Murashkin, E. V. Boltynjuk, R. Z. Valiev, and T. S. Orlova, J. Alloys Compd. **698**, 539 (2017).
[17]R. Haraguchi, Y. Yoshimatsu, T. Nagaoka, M. Arita, K. Edalati, and Z. Horita, J. Mater. Sci. **52**, 6778 (2017).
[18]H. Matsunaga and Z. Horita, Mater. Trans. **50**, 1633 (2009).
[19]M. Mito, H. Matsui, T. Yoshida, T. Anami, K. Tsuruta, H. Deguchi, T. Iwamoto, D. Terada, Y. Miyajima, and N. Tsuji, Rev. Sci. Instrum. **87**, 053905 (2016).
[20]D.-X. Chen and V. Skumryev, Rev. Sci. Instrum. **81**, 025104 (2010).
[21]W. A. Johnson and R. F. Mehl, Trans. Am. Inst. Metall. Pet. Eng. **135**, 416 (1939).
[22]M. Avrami, J. Chem. Phys. **9**, 177 (1941).
[23]H. Yinnon and D. R. Uhlmann, J. Non-Cryst. Solids **54**, 253–275 (1983).
[24]K. Barmak, Metall. Mater. Trans. A **41**, 2711 (2010).
[25]M. Castro, F. Dominguez-Adame, A. Sanchez, and T. Rodriguez, Appl. Phys. Lett. **75**, 2205 (1999).
[26]Y. Zhi-jie, D. Shu-e, W. Xiang-hui, and L. Pei-xia, Trans. Nonferrous Met. Soc. China **18**, 138 (2008).
[27]A. Grill, J. Horky, A. Panigrahi, G. Krexner, and M. Zehetbauer, Int. J. Hydrogen Energy **40**, 17144 (2015).
[28]C. Xu, Z. Horita, and T. Langdon, Acta Mater. **55**, 203 (2007).
[29]K. Edalati, A. Yamamoto, Z. Horita, and T. Ishihara, Scr. Mater. **64**, 880 (2011).